SEOP polarized ^{3}He Neutron Spin Filters for the JCNS user program

You may also be interested in:

A new fast detection system at the KWS-2 high-intensity SANS diffractometer of the JCNS at MLZ - prototype test
A Radulescu, N Arend, M Drochner et al.

Conceptual design of a polarized 3He neutron spin filter for polarized neutron spectrometer POLANO at J-PARC
T Ino, K Ohoyama, T Yokoo et al.

SEOP polarized ^{3}He Neutron Spin Filters for the JCNS user program

Earl Babcock[1*], **Zahir Salhi**[1], **Tobias Theisselmann**[1], **Denis Starostin**[1], **Johann Schmeissner**[1,2], **Artem Feoktystov**[1], **Stefan Mattauch**[1], **Patrick Pistel**[3], **Aurel Radulescu**[1], **Alexander Ioffe**[1]

[1] Jülich Centre for Neutron Science (JCNS) at the Heinz Maier-Leibnitz Zentrum (MLZ), Lichtenbergstaße. 1, 85747 Garching Germany

[2] *current* National Research Nuclear University MEPhi, Kashira Hwy, 31, Moscow, Russia, 115409

[3] Forschungszentrum Jülich GmbH ZEA-1, Leo-Brandt-Straße, 52425 Jülich Germany

E-mail: * e.babcock@fz-juelich.de

Abstract. Over the past several years the JCNS has been developing in-house applications for neutron polarization analysis (PA). These methods include PA for separation of incoherent from coherent scattering in soft matter studies (SANS), and online polarization for analysis for neutron reflectometry, SANS, GISANS and eventually spectroscopy. This paper will present an overview of the user activities at the JCNS at the MLZ and gives an overview of the polarization ^{3}He methods and devices used. Additionally we will summarise current projects which will further support the user activities using polarised ^{3}He spin filters.

1. Introduction

SEOP has long been proposed as a method for in-situ polarization of ^{3}He neutron spin filters (^{3}He NSF) and has now been realised at many centres worldwide [1–5]. Offline, or laboratory polarised ^{3}He NSF have also been used and refined to great success [6, 7]. However while being a simpler, albeit very robust, installation on the neutron instrument, these systems require continual maintenance to refresh the cell's polarization and often lead to the necessity of a ^{3}He service group which may or may not be available for all centres. Because of this, the long term strategy of the JCNS has been to focus on in-situ SEOP polarizers which are customised and integrated to each particular application, leading to long term stability, independence and scalability [8].

We currently have one long-time running in-situ polarizer developed for the MARIA magnetism reflectometer [9]. This system has undergone many upgrades to the lasers, magnetic cavity and heating system which will be the focus of an upcoming paper. It is used as the prototyping bed for other in-situ polarised applications for our institute such as for analysis on the SANS diffractometers KWS-1 and KWS-2 and for for incident beam polarization on a thermal time-of-flight spectrometer TOPAS [10–12]. The methods for standard polarized reflectometry and SANS using ^{3}He NSF analysis are "routine" as such instrument capabilities have been explored [13,14]. The goal of much of our program is to further develop the methods, and to increase the available Q-coverage of the analyzer systems over what is currently available to add to the scientific applications of the methods which were summarized in [15]. Finally the
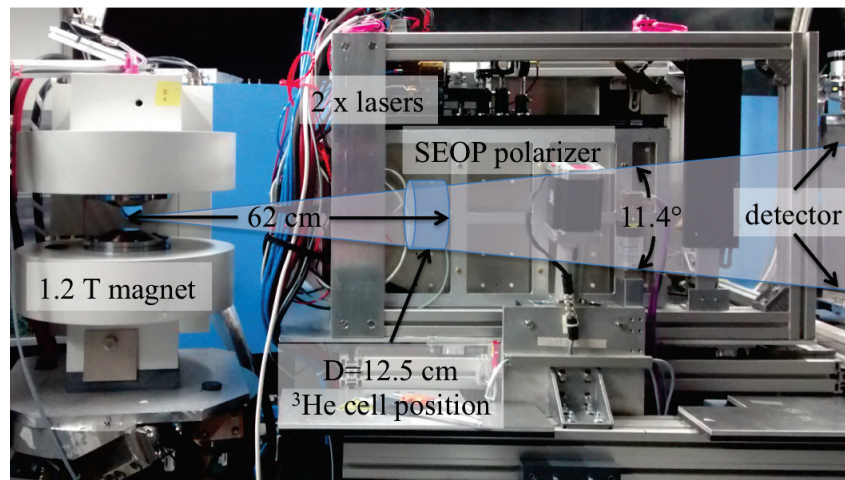
Figure 1. A picture of the current revision of the MARIA analyzer with the neutron/laser shielding box removed. The field geometry of the box is orthogonal to the 1.2 T sample magnet field (2.2 T with reduced pole-gap) in order to prevent magnetic coupling of the two systems. This along with the angled front yokes allow a closer approach of the front of the ^{3}He spin filter cell to the sample area, about 55 cm, thus increasing the angular-coverage or Q-range to over 11° or 0.23Å^{-1} for 4.5Å neutrons and a D=12.5 cm, L=8 cm cell. Above the box the two VBG narrowed lasers are mounted which are directed onto the cell with 3 mirrors.

system for TOPAS will also build upon the experience learned from the other devices, largely the MARIA analyzer, but will polarize the incident beam, which for the case of TOPAS's energy range and focusing guide geometry would not be possible with a super-mirror type device [12]. This paper will describe the complete MARIA analyzer and it's applications, as well as the KWS-1 and KWS-2 systems that are in production, giving concrete examples from user experiments. Then we will discuss the prototyping under way to provide in-situ polarization for each application to support the long term user needs.

2. MARIA polarization ^{3}He analyzer

Our current online SEOP system for MARIA, which will serve as the model for many other JCNS instruments such as KWS1, KWS2 and TOPAS, has many innovations. These innovations have been arrived upon over a long time with experience and testing of online SEOP polarizers for neutron instrumentation beginning with work on PF1B at the ILL and at ISIS [4, 16]. The beginning system for MARIA was essentially a further optimised version of these predecessors. However the system has continually evolved into its current state. The refinements cover every major subsystem of the device including: Python-based NMR and control program with web-GUI interface, upgraded laser systems, all-electric heating systems, new optimised magnetic field geometry and neutron spin transport. A detailed description of all of these devices will be the subject of a future instrument publication, here we will summarise each of these components and the overall performance characteristics of the final device. A picture of the MARIA analyzer system is given in figure 1.

NMR free induction decay (FID) and adiabatic fast passage (AFP) flipping are both available on all JCNS ^{3}He NSF systems. The FID allows one to monitor the ^{3}He polarzation over time and characterize the optical pumping parameters such as the spin-up time constant and cell lifetime. Our FID system conserves the phase information of the ^{3}He precession and thus also allows us to probe whether the ^{3}He is in the up or down state. It is a single-coil pulse and receive system

similar to that of [17] however using a house developed analogue switch and signal conditioning amplifier similar to [18]. The AFP allows the ^{3}He NSF to double as a high performance, wide area neutron flipper as well [19]. The AFP program is an all digitally generated pulse similar to that in [20], and amplified using a house built power amplifier with a 120 V$_{pp}$ output from 5 kHz up to 100 kHz. For the case of in-situ optical pumping via SEOP, the handedness of the circular polarization, and therefore the alkali-metal polarization, must be in phase with the direction of the ^{3}He spin. For this purpose we use liquid crystal variable wave retarders, which can be switched between $1/2\ \lambda$ and $1\ \lambda$ retardance by applying a TTL pulse to a house built analogue liquid crystal (LC) wave plate driver. For our system there are 3 mirrors at approximately 45° to steer the laser beams into the cell, each of which can cause a slight rotation of the plane of polarization. To compensate for this, we found it most robust to use the LC as a switchable $1/2$ to $1\ \lambda$ retarder and a fixed 0-order quartz $1/4\ \lambda$ at 795 nm retarder set to give net $1/4\ \lambda$ and $3/4\ \lambda$ retardances in conjunction with the effect of the mirrors to provide the resulting right and left handed polarizations of the pumping lasers. All the NMR devices and the switching of the LC retarders are accomplished with a program written in Python which has a web-browser interface that can be accessed remotely over a web server or via IP protocols. The program controls a 1.25 MHz Lab-view DAQ card using the National Instruments DAQmx 8.0 driver library which runs in either Linux or Windows.

Our laser systems have also been upgraded. Formerly diode array bars (DAB) with external cavities formed by plane-reflection diffraction gratings in a Littrow-type configuration were used [21] as narrow-band optical pumping light has been shown to provide the best SEOP performance. However continuation of this work has found a new method using chipped volume Bragg gratings, CVBG, to provide higher absolute ^{3}He polarizations [22]. Additionally CVBG narrowed lasers give higher laser output for the same power laser diode, and contain much fewer optical elements making the cavity more compact, stable and robust for long term operation when used in in-situ ^{3}He polarizer applications. A photo of the new laser cavity is shown in figure 2. In this photo the laser is shown mounted inside a newly designed compact box for mounting the laser and cavity optics, plus external connections to the current cables and cooling water. This box also provides environmental protection and increased laser security. Two of these lasers are used due to the large 0.85 litter volume of the ^{3}He NSF cell used on MARIA, however other applications using smaller volume cells will use only one.
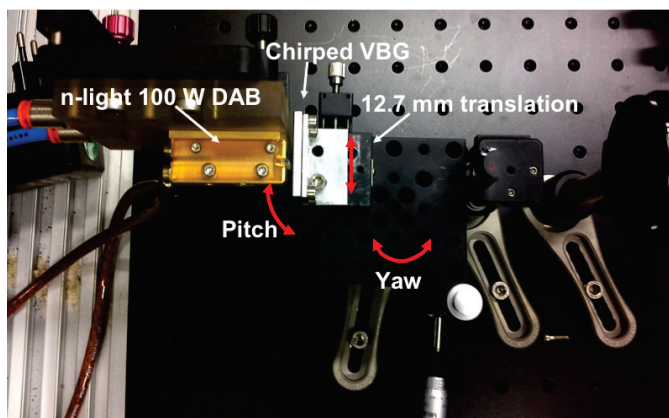

Figure 2. A picture of the current volume Bragg grating narrowed laser configuration on MARIA. This optical setup has now been adapted to fit in a custom made enclose box to enclose and mount all the optics and provide connections to power cable and cooling water.

As can be seen in figure 1 the magic box-style magneto-static cavity has also been updated and improved. The principle of operation remains the same to that of prior magic-boxes for online SEOP polarization [4,9] however the front set of magnetic "core-yokes" have been rotated by 45°. This modification accomplishes two things: one, the angled plates help shift the homogeneous region of the box forward towards the sample area, and two, they reduce the area of the opening
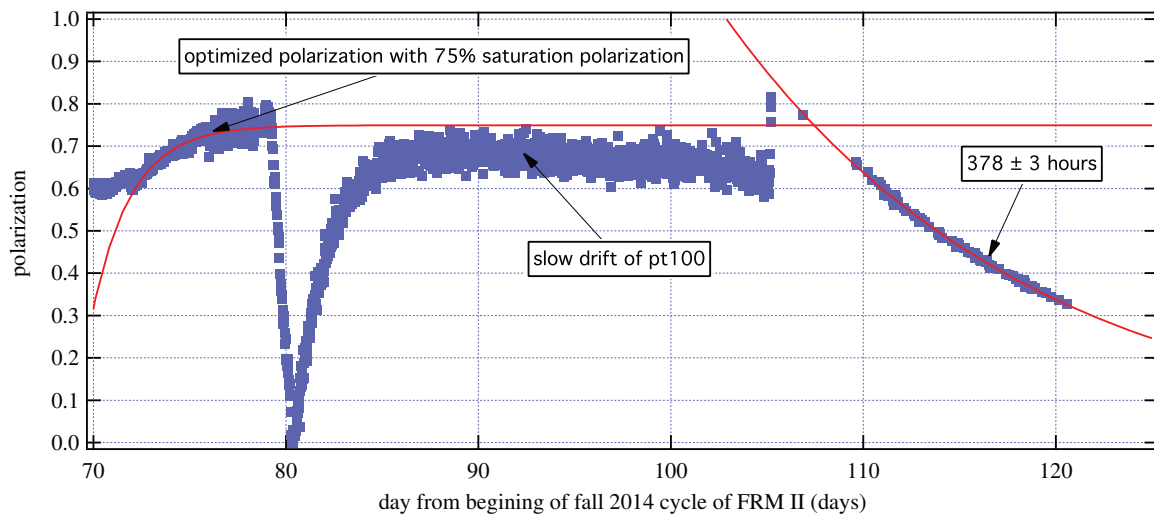
Figure 3. A graph of the MARIA analyzer ^{3}He polarization during the 18 October to 18 December 2014 cycle of the FRMII, days 75 to 105 on the graph. At the beginning of the shown data the system was re-optimised. At day 80 the system polarization was intentionally inverted with respect to the optical polarization and was polarised through 0. The slow degradation is caused by a long term degradation of the pt100 temperature sensor leads/connection. At the end of the data a room temperature T_1 lifetime measurement of the cell taken during a reactor pause can be seen. The measured T_1 is the same as was measured in laboratory conditions for this cell.

in the cavity on the side towards the sample magnet providing for better magnetic shielding from the field of it. This allows the cell to be moved closer to the sample, providing larger angular coverage for the same size cell. The cell used in MARIA, called Idefix [23], is 12.5 cm diameter and 8 cm long. In the revised magic box the front face of Idefix is about 27 cm from the magix box entrance, and 55 cm from the MARIA sample position providing a $\pm 5.7°$ angular coverage around the direct beam. Lastly, in comparison to the first revision of the MARIA analyzer [9] here we placed the magic box B_0 field orthogonal to that of the sample magnet. In the prior parallel-field geometry, the magnetic circuit of the magic-box was found to couple to the anti-parallel return flux of the sample magnet, causing zeo-field regions near the plane of the scattered neutron beam, leading to neutron beam depolarization before the ^{3}He NSF cell. This happens because the μ-metal of the magic box, when placed sufficiently close to the sample magnet, provides a high permeability return path for the sample magnet's flux that competes with the magnet's yoke. When explored with a hall probe, and also confirmed via finite element modelling of the coupled system, this essentially causes mirror images of the sample magnet coils to be formed inside the magic box above and below the symmetry axis of the beam, at sufficiently high sample magnetic fields, this then resulted in low field areas that partially depolarize the scattered neutron beam passing through these regions.

The orthogonal field geometry solves the problem of the coupling of the two magnetic systems. This insures that neutron spin transport is maintained at any sample filed, and the magnitude of the field at the position of the ^{3}He cell is stable to $1\text{x}10^{-4}$ or better (NMR frequency shifts of < 5 Hz) for any sample field from 1 mT up to the maximum of 1.2 T (with the standard pole-shoes installed). In this geometry the magic box can be placed very close to the sample magnet, however due to the requirement to rotate and tilt the sample environment, and

mechanics for a movable beam stop, plus radiation shielding/laser light shielding there is a space of approximately 10 cm between the perimeter of the sample magnet and the front face of the magic box. Therefore a short permanent magnet guide field, parallel to the sample magnet field is attached to the entrance window of the radiation-laser shield in order to maintain a minimum vertical neutron guide field of at least 10 G for all sample fields. The vertical field of this permanent magnet guide field overlaps sufficiently with the orthogonal field of the magic box such that 10 G is maintained everywhere and the neutron polarization rotates adiabatically for all neutron wavelengths used on MARIA which are ≥ 4.5 Å .

An un-anticipated benefit of this new construction is not only that the cell becomes closer to the sample position increasing its Q-range, but that the magnetic homogeneity has also improved. In the current cavity a recent room temperature T_1 measurement of the Idefix cell used for MARIA resulted in a value of 378±3 hours, the same value as was obtained in the laboratory for this cell [23]. This is an improvement compared to the prior simple rectangular magic box (L=80 cm W=30 cm H=40 cm with the field along the 40 cm direction and oriented parallel to the sample field) where the same cell obtained a $300 - 320$ hour lifetime depending on the sample field used. Since the currently measured lifetime in the MARIA system is within errors equal to the T_1 lifetime measurement of the same cell in laboratory conditions, the improvement is entirely attributed to improvement in the magnetic field homogeneity and improved shielding of the revised "angled-plate" magic-box magnetic cavity.

The overall performance is good and highly suitable for difficult user experiments. The SEOP ^{3}He NSF cell uses a hybrid Rb-K mixture to achieve high optical pumping efficiency [24,25] and has been prepared in house [23]. The Idefix cell has an internal diameter of 12.5 cm, length of 8 cm and a ^{3}He lifetime of 380 hours in laboratory conditions using a 6-coil, 2 m diameter and 2.5 m long, high homogeneity holding field. The details and preparation of the Idefix cell, as well as those of several other cells produced by us can be found in [23]. As stated earlier, inside the new MARIA magic-box this cell has a room temperature lifetime of 378 ±3 hours; this is more than sufficient to achieve high polarizations using the SEOP method.

The heating system has been upgraded from a heat-gun based, forced air approach to now use static air heated by electric cartidge heaters mounted in aluminium heat sinks. These stainless steel electric cartridge heaters (220 V CSS-series from Omega Engineering) now used for heating have not been found to decrease expected ^{3}He polarization, or room temperature T_1 lifetime. There is indeed some magnetic components to these heaters, namely the nickel plated lead wires, however in our installation, the two heaters are placed on ether side of the oven, inside the before mentioned aluminium heat-sinks, about 10 cm away from the cell, with the wires exiting away from the cell position. The aluminium heat sinks share are grounded to limit pickup of electrical noise by the NMR FID system.

Running at an oven temperature of approximately 185°C a saturation polarization of 70% is achieved in this cell. For this temperature in a hybrid cell [24] the spin exchange rate is slow; 50 hours for the Idefix cell used. The resulting polarization is highly stable at around 70% but this saturation polarization could be increased to 75% or more by by going to oven temperatures on the order of 20°C to 30°C hotter which would produce faster spin-up time constants. However, we will first install active temperature stabilization for the external enclosure of the device before pushing the parameters to the eventual limits.

In figure 3 the long term operation of the system can bee seen. In this particular data, it was run for over 160 days continuously, achieving a maximum 75% ^{3}He polarization value after a re-optimisation of cell temperature and laser tuning at around day 70 which was directly before the FRM II winter 2014 cycle that began at day 75 on the graph. During this 160 day span several user experiments have been performed. The time span of figure 3 particularly shows the ^{3}He polarization over the winter 2014 30-day half cycle from November 18th to December 18th 2014 and several weeks of a T_1 measurement over the reactor break from Dec 18th 2014 to Jan 13th
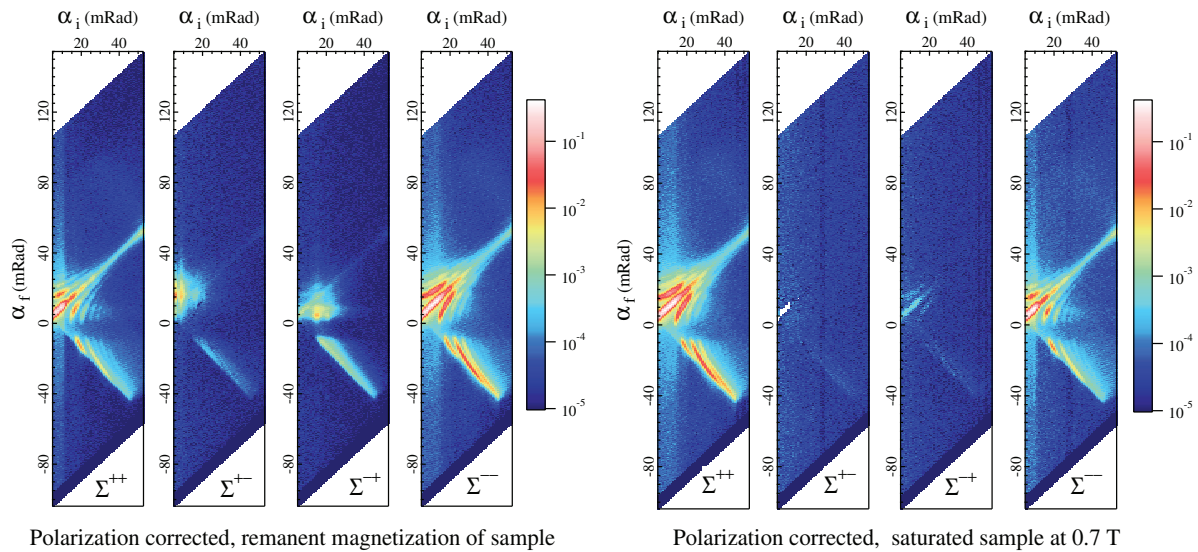
Figure 4. Polarised off-specular reflectivity data from the ^{nat}Fe^{58}Fe superlatice grating sample. An asymmetry in the spin-flip cross sections, graphs Σ^{+-} and Σ^{-+}, can be seen in the measurement at remanent magnetisation that disappears in the data to the right where an external 0.7 T field is applied. Note, the remnant field of the sample was anti-parallel to the applied field from the sample magnet. Close inspection of the diagonal spectral scattering shows a dynamic range of over 1×10^{-4} is achieved in the polarised mode. The data displayed are the normalised scattering cross-sections which have been corrected for the PA efficiencies.

2015. At the beginning of the data, the cell polarization was inverted and re-polarised through 0 (day 80) followed by a maximum of about 70% which slowly decayed due to a long term downward "drift" in temperature due degradation of the connections to our pt100 temperature sensor. Following this data the lasers and heating were shut off and a measurement of the cell T_1 lifetime can be seen. Subsequent to this data, the temperature sensor has been replaced by one with longer all platinum leads such that the connection of the pt100 to the temperature controller cable is outside the oven solving the problem of long term drift. For the spring 2015 FRM II reactor cycle the ^{3}He polarization was maintained constant for over 30 days during user experiments without any tuning of the lasers or oven temperature.

3. Examples from Reflectometry, GISANS and SANS data
In this section we will highlight some user measurements made with the ^{3}He NSF program at JCNS. As a test of polarization analysis on MARIA, a ^{nat}Fe^{58}Fe superlatice grating was measured. This sample had 10 repetitions of a ^{nat}Fe layer followed by a ^{58}Fe layer each of 0.1 μm thickness with a 10 μm period grating lithographically etched on the top surface. The sample was produced by the K. Temst group at KU Leuven [26], and was on loan from A. Wildes at the Insitut Laue-Langevin (ILL). Figure 4 shows α_f vs. α_i (final angle vs. incident angle) plots for the four polarization states at 1 mT (remanent) and 0.7 T (saturated) sample field. As can be seen in figure 4, rich off-specular scattering data can be obtained over a very large angular range and the specular reflectivity measured shows over a 1×10^4 dynamic range for the full polarization analysis mode. Before the 1 mT data the sample was magnetised anti-parallel to the neutron guide field and thus the remanent magnetization was anti-parallel to the neutron polarization for this data. One can see many orders of diffraction from the grating in the off-
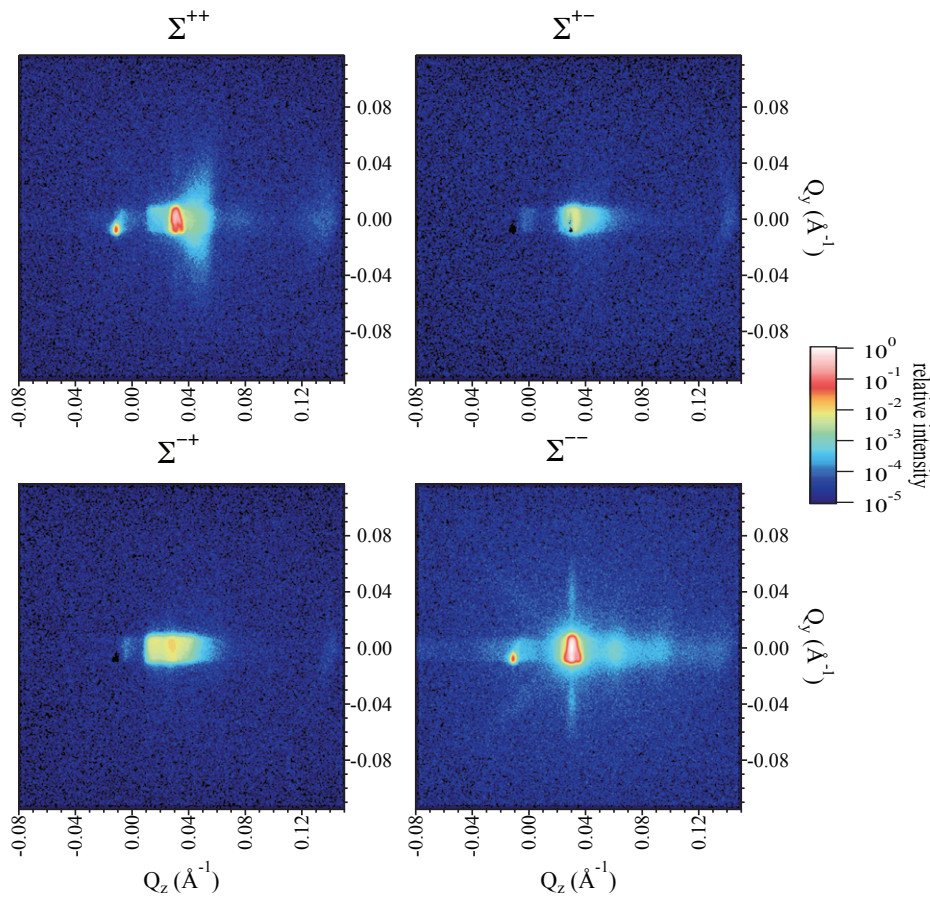
Figure 5. Full polarization analysis GISANS detector images from the magnetic multilayer (E. Kentzinger, et. al. MLZ proposal no. 10010) are shown. From the non spin-flip scattering in the Σ^{++} and Σ^{--} images, interfacial roughness is observed and from the spin-flip scattering in the Σ^{+-} and Σ^{-+} images, the GISANS from magnetic fluctuations is seen. The data was taken with 6 Å neutrons, the Q-values have a range of 0.230Å^{-1} for both the out of plane Q_z and in plane Q_x scattering corresponding to an angular coverage of $\pm 5.7°$. The detector was at an angle of $2°$ and the sample at an angle of $1°$ with respect to the direct beam. The data shown are normalized PA efficiency corrected cross sections.

specular data, further a spin-flip asymmetry can be observed in the remenant-magnetization measurement which disappears under magnetic re-orientation by the applied 0.7 T field.

The data shown in figure 4 have been corrected for the cell transmission and the polarizer, polarizer-flipper, and analyzer efficiencies following the methods which were clearly presented in [13]. In our case however, the procedure is somewhat simplified because the AFP ^{3}He flipper is an ideal neutron flipper [19], thus removing the inefficiency correction of the second flipper from the relations given in [13]. Further, for the current case of the in-situ polarizer on MARIA, the steady-state polarization means that time-dependent analyzing-power or transmission corrections are not needed when the system is in nominal operation. Work to model this data with the BornAgain project (i.e. software for simulations of GISANS and off-specular data using the DBW approximation) [27] as a model system is underway.

Another difficult application, polarization analysis with GISANS, is also possible. User

7

experiments of magnetic multilayers (E. Kentzinger, et. al.) at the JCNS for the MLZ proposal no 10010 are shown in figure 5. Spin-flip scattering in the GISANS data show the magnetic fluctuations in the sample and in the non spin-flip scattering one observes the interfacial roughness, GISANS is a unique way of separating these two effects. This work is a continuation of studies on such magnetic multilayers [28, 29], however the polarization analysis GISANS experiment is performed now for the first time. Again, the data shown in figure 5 has been normalized for the polarized [3]He NSF cell transmission and corrected for the polarizer efficiency, polarizer-flipper efficiency and [3]He NSF polarization efficiency again as above using the basic method of [13].
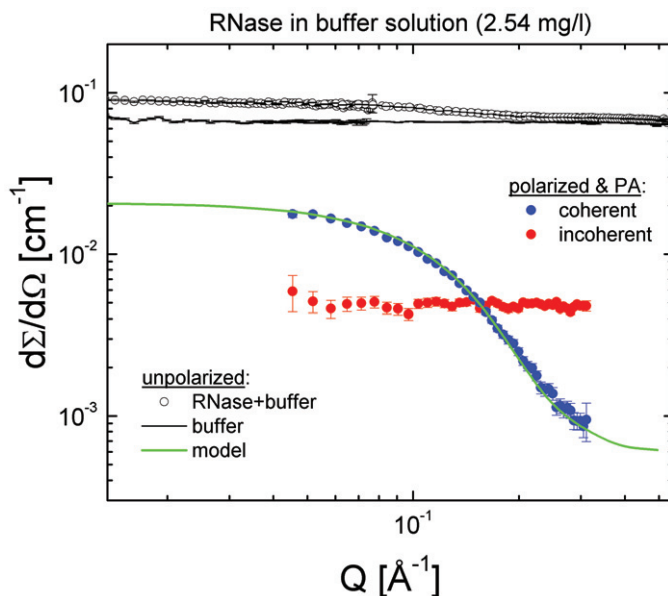

Figure 6. Polarised SANS data from an experiment by J. Fischer and R. Biehl. The unpolarised data for the Ribonuclease sample plus buffer solution and the buffer solution alone are at the top in black. One can see the scattering from the sample is only 10-20% above that of the buffer solution. Using polarization analysis the coherent scattering from the Ribonuclease sample is clearly obtained to a level 100 times below the total scattering, and 10 times below the level of innocent scattering of the Ribonuclease sample itself. The model-fit is also shown.

Lastly, a long proposed use of [3]He NSF is for the separation of coherent scattering from incoherent scattering scattering in soft matter studies [11, 15]. Work is continuing towards this goal, and more experiments have been done to further develop and refine the methods. Here we show one particular example of a user experiment. In this case a Ribonuclease sample is measured in a buffer solution, the data is shown in figure 6 [30]. One can see in the black curves at the top of the figure 6, corresponding to the unpolarised measurements of the sample in buffer and the buffer alone, that there is a large contribution from the buffer solution and the sample's own incoherent background. With the application of polarization analysis, seen in the colored data points, the coherent signal from the Ribonuclease can be clearly extracted to a level 100 times lower than the total scattering of the sample plus buffer, and to a factor of 10 times below the incoherent scattering of the Ribonuclease sample itself. In figure 6 the coherent form factor is compared to a calculated form factor based on the Ribonuclease A crystal structure including a hydration shell with 4% increased solvent density matches the absolute intensity of the coherent scattering [31]. This experiment was conducted with the provisional off-line polarised [3]He NSF cells and system described in [11] which is limited to a maximum Q-range of 0.3 Å^{-1} for a 4.5 Å incident neutron beam.

4. Planned in-situ devices for KWS1, KWS2 and TOPAS

For the two small angle scattering instruments at the JCNS in the MLZ, two very different in-situ polarizers are planned. The two instruments have different scientific focuses, KWS2 [15] being mainly soft matter for the separation of incoherent background, whereas KWS1 focuses

on magnetism research [10]. Soft matter studies will put highest priority on maximum Q-range whereas magnetism requires operation of the system in proximity to a high field sample magnet as on MARIA.

Therefore the system being built for KWS1 looks very similar to that on MARIA, but at 50% scale due to space constraints in the sample area for the sample magnet plus ^{3}He NSF analyzer system together. Further the mechanical design has been updated to be simpler and the length further shortened to 32 cm which was calculated to be the minimum possible for this style of magnetic cavity and still to have good performance. A diagram of the KWS1 design as optimised using a 3D FEM calculation which includes a model of the sample magnet is given in figure 7. The total length of the installation including the sample magnet will be under 1 m along the neutron beam to fit in the available sample environment space on KWS1. The magnetic cavity is currently under construction after which it will be tested first in the laboratory, and then on KWS1 using offline polarised ^{3}He NSF cells.
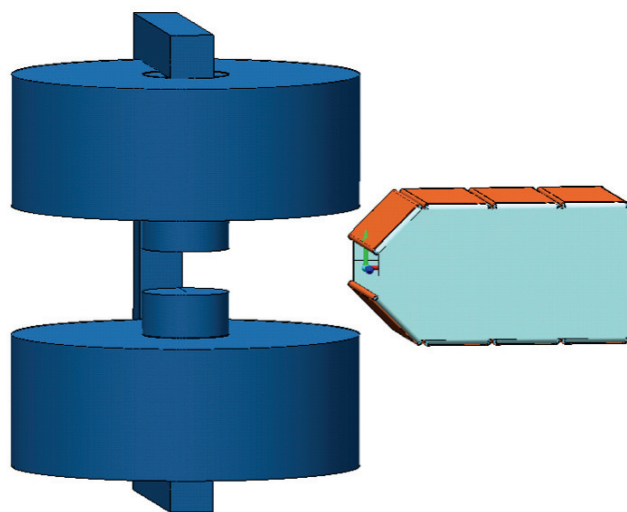

Figure 7. A diagram of the KWS1 magnetic system, similar to that on MARIA, as used to calculate the magnetic fields and compatibility. This system is designed to provide a similar angular coverage, up to $\pm 6.5°$ or $Q \leq 0.16 \text{Å}^{-1}$ using 4.5 Å incident neutron wavelength. The total length will be under 1 m along the neutron beam. Not shown is the laser and optics which will be mounted above the cavity as on MARIA.

The KWS2 analyzer will look much different as the goal is to place the sample as close as possible to the cell to increase the possible Q-range. Additionally the system must minimise the total length so as not to increase the effective minimum sample to detector distance because again, as for KWS1, the system will be placed in the sample environment area, between the sample and the detector tank. The KWS2 system will use a very compact solenoid cavity which has been described in previous proceedings [11]. The total length of this solenoid is 18 cm and allows a sample to be placed within 3 cm of the front of the ^{3}He NSF cell. This magnetic cavity has been constructed and tested for ^{3}He polarization lifetime: the lifetime of a test cell was measured to be about 400 hours, giving a magnetic relaxation term of approximately 1000 hours for the cavity. This value is again more than sufficient for in-situ polarization. The oven and heating system have also been prototyped. This system will undergo further testing, optimisation and mechanical refinement before eventual user operations.

The TOPAS in-situ polarizer will be the neutron polarizer for the incident beam. Thus a much more conservative approach is taken. A simple rectangular SEOP magic-box style magnetic cavity will be used very similar to those in [4, 9]. The box design has been resized for the smaller beam diameter required for an incident beam of about D=6 cm. The resulting cavity is 30 cm tall by 20 cm wide and 50 cm long. the field will be along the 30cm direction and be co-linear with the guide fields of TOPAS to prevent depolarization of the very fast 0.7 Å minimum neutron wavelength to be used there. Two VBG narrowed DAB lasers as mentioned
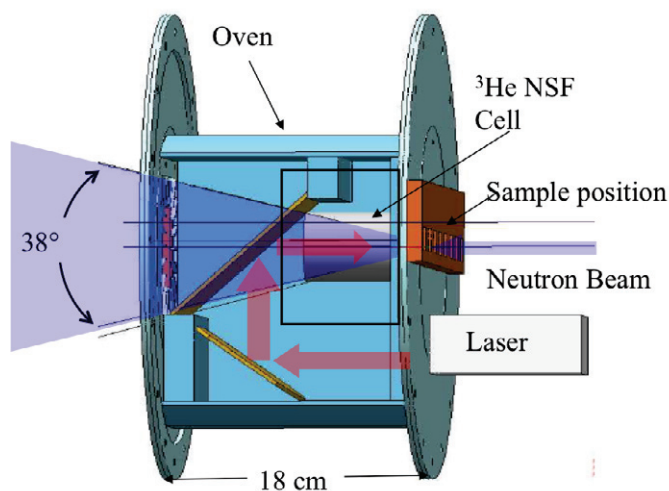
Figure 8. A diagram of the KWS2 magnetic system, SEOP oven and optics. The main components of the system have been prototyped and tested. Further mechanical optimisation and neutron testing will be conducted before routine use.

before will be used, one for the front 7.5 cm and the other for the back 7.5 cm of the 15 cm long cell needed to polarised the TOPAS incident beam. The magnetic cavity is nearing completion and will be tested soon. Several ^{3}He NSF cells with 3 bar ^{3}He and 6 cm diameter and 15 cm length have been produced and tested for lifetime, lifetimes in excess of 200 hours are achieved.

For the TOPAS analyzer, an offline polarised banana-shaped cell will be used in conjunction with a magic-PASTIS magnetic system. This device is described more fully in a separate paper in this same proceedings issue [32].

5. Conclusions and acknowledgements

The program for in-situ SEOP ^{3}He NSF at the JCNS at the MLZ has made many advancements. Several systems are in construction or testing phases and a working prototype has been in use on MARIA for several reactor cycles and corresponding user experiments. In total, four unique in-situ SEOP polarizers are currently planned for the JCNS instrument suite. These include the readily available MARIA analyzer, analyzer for KWS1 (in production) and polarizer for the incident beam on TOPAS (in production) all of which utilize a magic-box rectangular mu-metal magnetic capacitor geometry, and KWS2 (in testing) which uses an ultra compact solenoid geometry.

References

[1] Hayashida H *et al* 2014 *J. Phys.: Conf. Ser.* **528** 012020 (proc. of NOP&D 2013)
[2] Jones G *et al* 2006 *Physica B-Condensed Matter* **385-86** 1131–1133
[3] Tong X *et al* 2012 *Rev. Sci. Inst.* **83**
[4] Boag S *et al* 2009 *Physica B-Condensed Matter* **404** 2659–2662
[5] Chupp T *et al* 2007 *Nuclear Instruments and Methods in Physics Research Section A* **574** 500–509
[6] Chen W *et al* 2014 *J. Phys. Conf. Ser.* **528** 012014
[7] Andersen K *et al* 2009 *Physica B-Condensed Matter* **404** 2652–2654
[8] Babcock E and Ioffe A 2011 *Physica B-Condensed Matter* **406** 2448–2452
[9] Babcock E, Mattauch S and Ioffe A 2011 *Nuclear Instruments and Methods in Physics Research Section A* **625** 43–46
[10] Feoktystov A *et al* 2015 *J. Appl. Cryst.* **48** 61–70 URL http://dx.doi.org/10.1107/S1600576714025977

[11] Babcock E *et al* 2013 *Physics Procedia* **42** 154–162
[12] Voigt J, Babcock E and Brueckel T 2010 *J. Phys. Conf. Ser.* **211** 012032
[13] Wildes A 1999 *Rev. Sci. Inst.* **70** 4241–4245
[14] Krycka K, Chen W, Borchers J, Maranville B and Watson S 2012 *J. Appl. Cryst.* **45** 546–553
[15] Ioffe A *et al* 2012 *Chinese J. Phys.* **50** 137–154
[16] Babcock E *et al* 2009 *Phys. Rev. A* **80** 033414
[17] Parnell S, Woolley E, Boag S and Frost C 2008 *Meas. Sci. & Tech.* **19** 045601
[18] Babcock E 2005 *Spin-exchange optical pumping with alkali-metal vapors* Ph.D. thesis University of Wisconsin-Madison section 3.6.1
[19] Babcock E *et al* 2007 *Physica B-Condensed Matter* **397** 172–175
[20] McKetterick T *et al* 2011 *Physica B-Condensed Matter* **406** 2436–2438
[21] Babcock E, Chann B, Nelson I and Walker T 2005 *Applied Optics* **44** 3098–3104
[22] Chen W, Gentile T, Ye Q, Walker T and Babcock E 2014 *J. Appl. Phys.* **116** 014903
[23] Salhi Z, Babcock E, Pistel P and Ioffe A 2014 *J. Phys. Conf. Ser.* **528** 012015
[24] Chen W, Gentile T, Walker T and Babcock E 2007 *Phys. Rev. A* **75** 013416
[25] Babcock E, Chann B, Walker T, Chen W and Gentile T 2006 *Phys. Rev. Lett.* **96** 083003
[26] Temst K 2015 KU Leuven personal page for K. Temst http://www.kuleuven.be/wieiswie/en/person/00016278
[27] Durniak C, Pospelov G, Van Herck W and Wuttke J 2015 BornAgain *Software for simulating and fitting X-ray and neutron small-angle scattering at grazing incidence* http://www.bornagainproject.org
[28] Kentzinger E *et al* 2007 *Physica B-Condensed Matter* **397** 43–46
[29] Kentzinger E, Ruecker U, Toperverg B, Ott F and Brueckel T 2008 *Phys. Rev B* **77**
[30] Fischer J, Biehl R, Hoffmann B and Richter D 2013 *European Biophysics J. with Biophysics Lett.* **42** S65
[31] Svergun D *et al* 1998 *Proc. of the National Academy of Sciences of the United States of America* **95** 2267–2272
[32] Salhi Z *et al* 2015 *J. Phys. Conf. Ser.* **this issue**